Biochemical and Biophysical Research Communications 430 (2013) 1011–1015

Contents lists available at SciVerse ScienceDirect

Biochemical and Biophysical Research Communications

journal homepage: www.elsevier.com/locate/ybbrc

Catalytic efficiency of dehaloperoxidase A is controlled by electrostatics – application of the vibrational Stark effect to understand enzyme kinetics

Gal Schkolnik [a,b], Tillmann Utesch [a], Junjie Zhao [b], Shu Jiang [b], Matthew K. Thompson [b], Maria-Andrea Mroginski [a], Peter Hildebrandt [a], Stefan Franzen [b,*]

[a] Technische Universität Berlin, Institut für Chemie, Sekr. PC14, Straße des 17, Juni 135, D-10623 Berlin, Germany
[b] Department of Chemistry, North Carolina State University, Box 8204, Raleigh, NC 27695-8204, United States

ARTICLE INFO

Article history:
Received 28 November 2012
Available online 19 December 2012

Keywords:
Vibrational Stark effect
Hemoglobin
4-mercaptobenzonitrile
Enzyme kinetics
Electric field

ABSTRACT

The vibrational Stark effect is gaining popularity as a method for probing electric fields in proteins. In this work, we employ it to explain the effect of single charge mutations in dehaloperoxidase-hemoglobin A (DHP A) on the kinetics of the enzyme. In a previous communication published in this journal (BBRC 2012, 420, 733–737) it has been shown that an increase in the overall negative charge of DHP A through mutation causes a decrease in its catalytic efficiency. Here, by labeling the protein with 4-mercaptobenzonitrile (MBN), a Stark probe molecule, we provide further evidence that the diffusion control of the catalytic process arises from the electrostatic repulsion between the enzyme and the negatively charged substrate. The linear correlation observed between the nitrile stretching frequency of the protein-bound MBN and the catalytic efficiency of the single-site mutants of the enzyme indicates that electrostatic interactions play a dominant role in determining the catalytic efficiency of DHP A.

1. Introduction

Dehaloperoxidase-hemoglobin A (DHP A) is a predominantly monomeric [1] bifunctional protein found in the benthic organism *Amphitrite ornata* [2,3]. The protein, also called DHP for sake of brevity, appears to have a globin-peroxidase double function [4,5]. In its peroxidase function it can oxidize the marine toxin 2,4,6-tribromophenol (TBP) to 2,6-dibromoquinone (DBQ), a less toxic compound [5]. It can also similarly oxidize all the other 2,4,6-trihalophenols, including environmental pollutant 2,4,6-trichlorophenol (TCP) [6,7], and thus has the potential to serve as a bioremediation enzyme. Fig. 1 shows the reaction catalyzed by DHP at physiological pH of 7.4. Given that pKa of TCP is 6.2, the majority of the substrate molecules are negatively charged under physiological conditions [8]. In a previous study [9] it has been found that the isoelectric point of the DHP protein is pI = 6.8, indicating that at physiological pH it too has an overall negative charge. The charge-charge repulsion between the substrate and enzyme may explain the observation that the rate constants for substrate oxidation are dominated by diffusion rather than electron transfer, which was deduced previously from a temperature-dependent analysis of a Michaelis–Menten model for peroxidase kinetics [10]. The combination of the observation of diffusion control for the oxidation process and the mutual repulsion of the negatively charged enzyme and substrate suggests that the electrostatic potential at the protein surface should have a substantial effect on the catalytic rate. In previous work DHP A mutants were studied consisting of substitutions that alter the total charge of the protein by up to one unit of charge, including R33Q, K36A (positive to neutral), N91K (neutral to positive), N61D and N96D (neutral to negative) [9]. The mutation positions were located in a belt that encircles the heme pocket (see Fig. 4). Both the measured pI and ionic strength effect on kinetics strongly suggest that the protein is slightly negatively charged at pH = 7.0 [9], so that all of the above mutations correspond to an increase in the overall negative charge of the protein, except for N61K in which the total negative charge is decreased. These single charge mutations result in a decrease in the catalytic efficiency of the enzyme, expressed as k_{cat}/K_m, with the exception of N61K, which results in an increase in k_{cat}/K_m. The observed trend in the surface mutations was rationalized by the observation that both enzyme and substrate are negatively charged, creating mutual repulsion. Based on the dependence on ionic strength, it was concluded that the process is electrostatically controlled [9]. In the present study, we test this conclusion with the aid of the labeled protein that features a probe molecule sensitive to the electric field at the surface of the protein.

The vibrational Stark effect (VSE) describes the sensitivity of certain vibrational modes to local electric fields, according to the following equation:

$$\nu = \nu_0 - \Delta\vec{\mu}\cdot\vec{F} - \frac{1}{2}\vec{F}\cdot\Delta\vec{\alpha}\cdot\vec{F} \quad (1)$$

* Corresponding author. Fax: +1 919 515 8909.
E-mail address: Stefan_Franzen@ncsu.edu (S. Franzen).

0006-291X/$ - see front matter © 2012 Elsevier Inc. All rights reserved.
http://dx.doi.org/10.1016/j.bbrc.2012.12.047

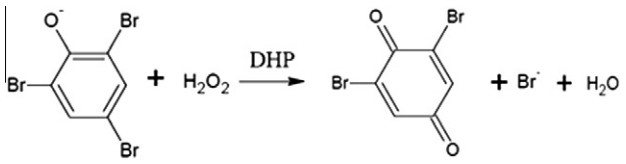

Fig. 1. The reaction catalyzed by DHP in its role as peroxidase.

where v and v_0 are the vibrational frequencies of a certain vibrational mode in the presence and in the absence of an electric field $\vec{F}$, respectively, $\Delta\vec{\mu}$ is the difference dipole moment of the mode, also known as the Stark tuning rate, and $\Delta\vec{\alpha}$ is its difference polarizability [11–13]. For many cases, the linear term has been shown to suffice to describe the VSE [14–16], providing a potentially powerful tool for indirect electric field measurements using a variety of vibrational spectroscopies [17]. While cyanide has been used as an internal probe, thiocyanate has also been used as a surface probe of the electrostatics of protein–protein interaction [18] and a number of non-natural amino acids have been introduced with a variety of functional groups for VSE measurements [19]. Recent studies of nitriles in solution show a correlation between the measured Stark tuning rate and the Onsager reaction field [20].

In this study, several of the DHP A mutants previously studied in kinetic assays [9] were labeled with 4-mercaptobenzonitrile (MBN), a VSE probe molecule [14,16,21,22], by covalently binding it to C73, the only surface cysteine in DHP A [23]. Since the average solvent environment is relatively constant, the differential effect on the frequency of the MBN probe is hypothesized to be entirely due to changes in the protein surface for each mutant. The vibrational frequency of the MBN nitrile stretch was measured for each variant, to probe the local electric field on the protein surface, at the label location. Molecular dynamics (MD) simulations were performed to supply further information concerning label position and protein electrostatics. The nitrile stretching frequency of the protein-attached MBN was plotted against the previously reported [9] catalytic efficiency of the variants leading to conclusions regarding the relation between DHP A electrostatics and kinetics.

2. Materials and methods

For the procedure of mutant production and purification, see Supplementary Information.

After protein purification and oxidation using excess potassium ferricyanide, a small excess of KCN was added to the mixture, so that the cyanide irreversibly bound to the heme, in order to avoid any uncontrolled changes to the oxidation state of the heme. Oxidation state as well as cyanide binding were verified using UV/Vis spectroscopy (see SI). A 100-fold molar excess of MBN dissolved in DMSO was added to the protein solution. The mixture was shaken overnight at 4 °C. Centrifugation at 4800*g* was used to separate the protein-containing aqueous phase from the fraction of precipitated MBN. This step was repeated at least three times, or until no more precipitate could be visually detected. Subsequently, the supernatant was dialyzed against potassium phosphate buffer, 10 mM, pH = 7.0, in order to remove any residual unbound label, as well as for buffer exchange.

FTIR measurements were performed in a split-beam cell for liquid samples (path length 25 μm) equipped with CaF_2 windows, using a Digilab FTS-6000 spectrometer with a MCT detector. The spectral resolution was 2 cm^{-1}. The spectrometer was purged with dry air. 1000–1500 scans were accumulated for each spectrum. For measurement of labeled DHP mutants, the split beam cell was loaded with the labeled wild type (WT) protein in one compartment and a labeled mutant in the other, to enable comparison of the MBN nitrile stretching frequency in the mutant with that of the WT protein. A spectrum of the split beam cell compartment loaded with the relevant buffer was used for background subtraction, to obtain an absorption spectrum. The MBN nitrile stretching band position was determined by Gaussian peak fit, after baseline subtraction of the absorption spectrum. Each mutant was measured five times and averaged. The standard deviation was determined to be ±0.1 cm^{-1}.

To analyze the structural fluctuations and resulting changes in the electrostatic properties, molecular dynamics (MD) simulations of five single mutants (R33Q, K36A, N61D, N61K and N96D) and the wild type enzyme were carried out. The initial coordinates of the six models were extracted from the crystallographic structure derived from the PDB structure 2QFK. The desired mutations were incorporated with the psfgen tool integrated in VMD [24]. All models were modified with an MBN label at position 73 and with a cyanide ligand occupying the free coordination site at the heme. The modified protein was solvated in a ca. $60 \times 60 \times 50$ $Å^3$ large TIP3P water box [25] with an ionic strength of ca. 10 mM mimicked by Na^+Cl^-. The protein side chains were protonated according to pH 7.0. The heme adjacent H55 was protonated at its N_ε as described recently [26]. All particles were treated with the CHARMM 27 force field [27] extended with parameters for the CN and MBN derived from DFT calculations, which are discussed in the Supplementary Information.

Before running the production dynamics, the models were prepared by an energy minimization of 10,000 steps with the conjugated gradient, a heating procedure to reach 300 K and a water equilibration of 60 ps. During these steps, initial position restraints of 25 kcal mol^{-1} $Å^{-2}$ on all heavy atoms were stepwise decreased until all atoms were allowed to move freely. Afterwards, 10 ns long MD simulations were performed and parameters such as distances, angles and dipole moments were evaluated every 50 ps. All simulations were carried out with NAMD 2.7 [28] under periodic boundary conditions and at constant pressure and temperature (NPT) facilitated by Langevin piston dynamics [29]. The time step of 2 fs was enabled by freezing all bonds containing hydrogen atoms with the RATTLE algorithm [30]. Short-ranged electrostatics and van der Waals interactions were truncated at 12 Å, while long-ranged electrostatics were calculated with the particle Mesh Ewald summation [31]. Simulations were run twice for N61D, to examine reproducibility. The figures contain both N61D runs, for reference.

3. Results and discussion

3.1. FTIR spectra of MBN-labeled mutant and wild type DHP A

The FTIR absorption spectrum of labeled wild-type (WT) DHP A after baseline subtraction is shown in Fig. 2. A heme-bound cyanide stretching mode, originating from the KCN added to the protein solution after oxidation, is detected at 2128.3 cm^{-1}. The nitrile stretch arising from the MBN label covalently bound to Cys73, the only surface cysteine found in DHP A, is seen at 2234.9 cm^{-1}. This frequency is characteristic of aromatic nitriles in a protic environment [14,32–34], indicating that the MBN is exposed to the aqueous phase while attached to the protein surface. This is confirmed by MD simulations, see, e.g., Fig. S1. No signal that could be assigned to non-specifically bound MBN was detectable in any of the spectra. Each protein variant was measured five times, with a root mean standard deviation of ±0.1 cm^{-1} for the reported peak frequencies.

The single charge mutations have resulted in small but reproducible and statistically significant changes in the nitrile stretching frequency of the protein-bound MBN, in the mutants compared to WT DHP A. These frequency changes are inversely correlated to the

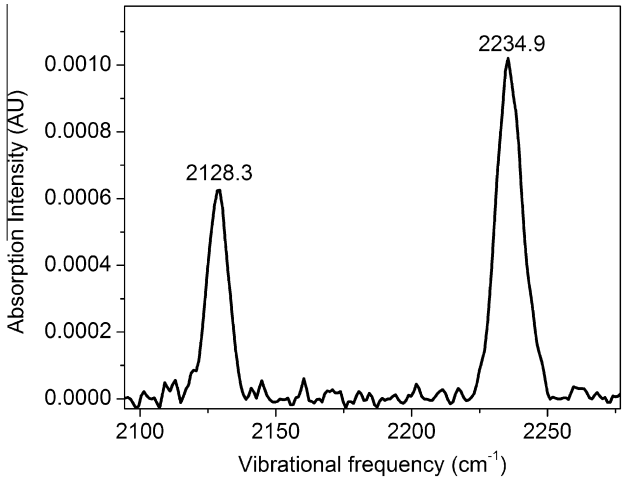

Fig. 2. Baseline subtracted FTIR absorption spectrum of MBN-labeled wild type DHP A, displaying the heme-bound cyanide stretch at 2128.3 cm^{-1}, and the nitrile stretch of MBN covalently bound to C73, at 2234.9 cm^{-1}.

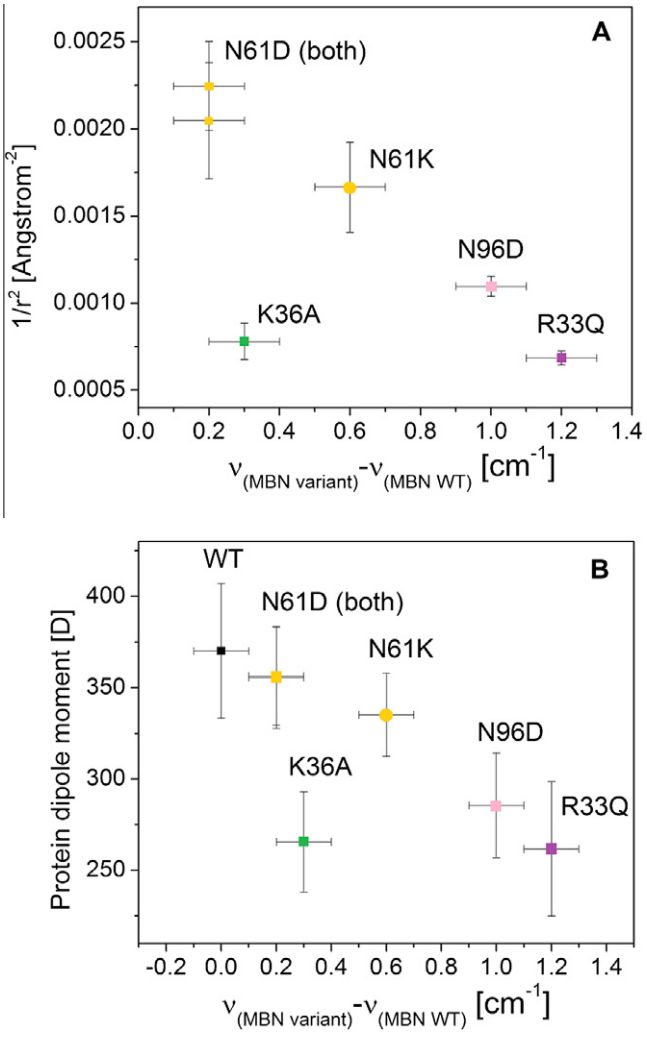

Fig. 3. (a) Variation of the difference of the nitrile stretch frequency between the mutants and the wild type protein with $1/r^2$, where r is the distance from the charge mutation site to the MBN nitrile bond, **(b)** Protein dipole moment vs. the change in nitrile stretch frequency between the WT and variant proteins. All data refers to DHP A with heme-CN and MBN attached to Cys73. Frequencies were determined by FTIR, and the rest of the data was obtained by MD simulations.

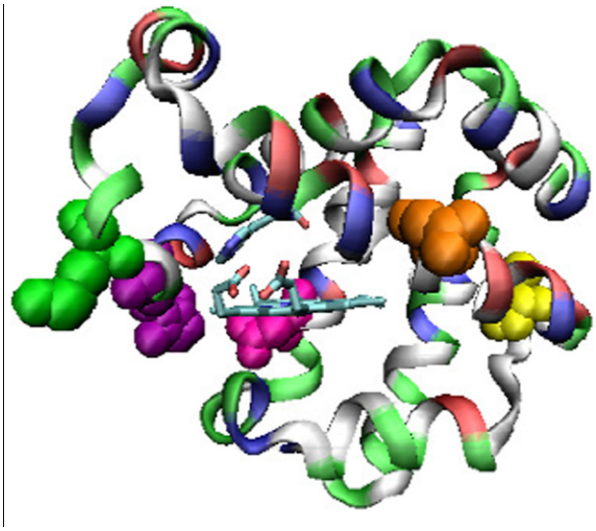

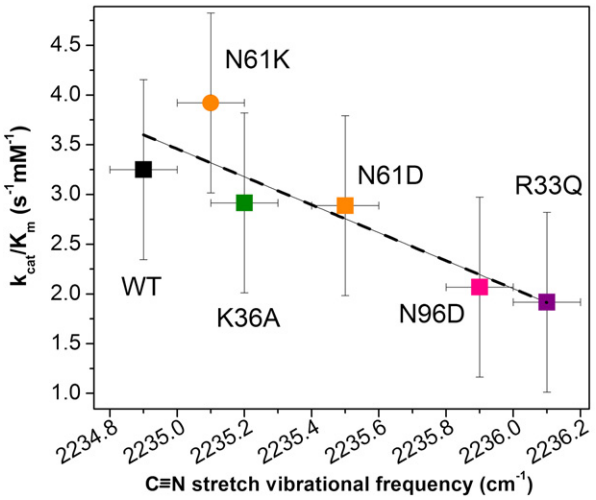

Fig. 4. Top: DHP A with several positions highlighted (Crystal structure 3LB2 [36]). Yellow: Cys 73, the MBN covalent-binding position. Mutation positions: 33 purple, 36 green, 61 orange, 96 pink. **Bottom:** k_{cat}/K_m (catalytic efficiency) vs. the nitrile stretching frequency. The color code corresponds to the top figure. Orange circle: N61K, orange square: N61D and black square: WT DHP A. Dashed line: linear fit, $k_{cat}/K_m = 3144.7–1.4\nu_0$, $R^2 = 0.73$. (For interpretation of the references to color in this figure legend, the reader is referred to the web version of this article.)

square of the distance between the MBN nitrile bond and the mutation site (r^2), and linearly correlated to the protein dipole moment, both calculated by MD simulations. These correlations are presented in Fig. 3 A and B, respectively. The correlations hold for all variants, except for the one with a charge mutation in position 36, a position that shows a much greater conformational flexibility than the other mutation positions, as reflected in the MD root mean square fluctuation (rmsf) graph shown in Fig. S2 (top). Since the electric field caused by a single charge varies proportionally to $1/r^2$, where r is the distance from the charge, the correlation between the changes in the MBN nitrile stretch frequency and this parameter indicates that the VSE probe can indeed sense the change to the protein electric field caused by a single charge mutation over considerable distances (21–38 Å). Such sensitivity on the nm range has also been demonstrated previously [21]. The observation that the MBN nitrile stretching frequency is linearly correlated to the protein dipole indicates that it reflects changes to overall protein electrostatics. These two last observations are strengthened by comparing the difference in the MBN nitrile stretching frequency observed for N61D and N61K in 150 mM

Table 1
MBN nitrile stretching frequencies, label distance from mutation site, protein dipole and electric fields obtained for the different DHP A variants.

DHP A variant[a]	ν_{MBN} (cm^{-1})[b]	Protein dipole (D)[c]	d_{label} (Å)[d]	Mut-$C_{(MBN)}$-$N_{(MBN)}$ angle (deg)[e]	$E_{F,MBN}$ (V/m) [f]
WT	2234.9	260 ± 40			3.2×10^8
R33Q	2236.1	270 ± 30	38 ± 1	142 ± 15	5.1×10^8
K36A	2235.2	340 ± 20	36 ± 2	135 ± 18	3.6×10^8
N61D	2235.5	360 ± 30	22 ± 2	118 ± 18	4.1×10^8
N61K	2235.1	290 ± 30	25 ± 2	120 ± 20	3.4×10^8
N96D	2235.9	370 ± 40	30 ± 1	152 ± 13	4.8×10^8
N61D (KPB 150 mM)	2235.4				4.0×10^8
N61 K (KPB 150 mM)	2235.5				4.1×10^8

[a] Unless stated otherwise, measurements were performed at a potassium phosphate buffer concentration of 10 mM, pH = 7.0.
[b] MBN nitrile stretching frequency. Average over five measurements, root mean standard deviation = ±0.1 cm^{-1}.
[c] Protein dipole, according to MD simulations.
[d] Mutation site distance from MBN nitrile bond center, according to MD simulations.
[e] Angle between the mutation site, the MBN carbon and the MBN nitrogen, from MD simulations.
[f] Electric field at the MBN nitrile, in mean nitrile bond direction, calculated according to the linear term of Eq. (1).

potassium phosphate buffer (pH = 7.0), to that observed in 10 mM buffer. In the higher ionic strength buffer the MBN nitrile stretch is found at statistically identical frequencies for the two variants, whereas in lower ionic strength they are separated by 0.4 ± 0.1 cm^{-1} (see Table 1). The lack of shift in the vibrational frequency due to the screening of the local field in high ionic strength media is consistent with other data since MBN nitrile is located at distances ranging from 22 to 38 Å from the sites of the various mutants so ionic strength would be expected to have a significant effect (Table 1). The linear term in Eq. (1) can be used to determine the electric field experienced by the MBN nitrile, in the nitrile bond direction, for each DHP A variant. For ν_0, 2233.3 cm^{-1} is used (see SI). The Stark tuning rate ($\Delta\vec{\mu}$) used here for the protein-bound, buffer exposed MBN is 6.0×10^{-9} cm^{-1}/V/m [14]. The electric fields calculated using these parameters range from 3.2×10^8 to 5.1×10^8 V/m. All the above mentioned measured and calculated values appear in Table 1.

It is interesting to note, that while the Stark tuning rate for heme-bound cyanide (hereafter heme-CN) is not expected to be significantly lower than that of MBN [35], the changes to its stretching frequency in the mutants compared to the WT protein are small relative to the changes observed for the MBN nitrile (See Table S2). Additionally, they do not correlate with either $1/r^2$, where r is the distance of the CN bond of the heme-CN from the charge mutation, nor with the protein dipole moment (see Fig. S3). These observations are explained by the angle between the heme-CN nitrogen, its carbon and the mutation site (Mut-C-N angle, explained in Fig. S2, bottom) predicted by MD simulations, and shown in Table S2. Since these angles are close to 90°, the product of the scalar multiplication in the linear term of Eq. (1) becomes small. Therefore, changes to the electric field due to charge mutations become smaller, and their dependence on r^2 or the protein dipole moment becomes statistically insignificant.

3.2. Connecting Stark label vibrational frequency and kinetic findings in DHP A

Having established, with the aid of MD simulations, that the changes to the MBN-nitrile frequency in the charge mutants compared to the WT DHP A indeed reflect changes to overall protein electrostatics, one may compare the present findings to the kinetic data for the same single-charge surface mutants [9]. When plotting the frequency changes against the catalytic efficiency of the enzyme, (Fig. 4), a linear correlation is observed. The correlation between the catalytic efficiency (k_{cat}/K_m) and the MBN-nitrile vibrational frequency, which as explained above reflects the overall change in protein electrostatics, clearly indicates that the mutations investigated here preferentially affect the catalytic efficiency of DHP A by changing its overall electrostatics rather than by structural or functional alterations to the active site.

Because in DHP A the rate of enzymatic turnover is controlled by diffusion, particularly at low substrate concentrations, the electrostatic effect observed here may be attributed to the potential experienced by the substrate as it approaches its as yet unknown binding site [2,26]. This observation is confirmed by the decrease in the catalytic efficiency of WT DHP A when the reaction is performed at a lower ionic strength [9]. Further, the effect of charge mutations on the MBN nitrile stretching frequency sharply decreases upon increasing the buffer concentration from 10 to 150 mM (Table 1). It thus appears that ionic screening plays an important role in both DHP A kinetics and in the charge-mutation-induced change to the vibrational frequency of the VSE probe, confirming that enzyme kinetics are controlled by the electrostatic interaction between the charged substrate and the overall electric field of the enzyme.

This study demonstrates that VSE can be used to probe the effect of the overall protein electric field on an enzymatic process. Our results confirm the previously observed relation between DHP A kinetics and electrostatic changes due to charge mutations in the vicinity of its heme-pocket, while experimentally disentangling the role of protein electrostatics from possible mutation-induced structural and functional changes.

In a wider context, the present results suggest that electrostatic control may be an important factor in steering substrates towards enzyme active sites in biochemical pathways. The method presented here therefore can be useful in the future for the measurement of the effect of protein surface electrostatics on enzyme function, particularly in processes where the binding of a charged substrate may be a rate limiting step in the catalysis. Considering that many enzymes have charged substrates, such a method has potentially wide application in biophysics.

Acknowledgments

Financial support by the German Research Foundation (DFG) in the framework of the IGRTG 1524 is gratefully acknowledged. We would like to thank HRLN for computer resources and UniCat for financial support. SF thanks the ARO for support through grant LS-57861.

Appendix A. Supplementary data

Supplementary data associated with this article can be found, in the online version, at http://dx.doi.org/10.1016/j.bbrc.2012.12.047.

References

[1] M.K. Thompson, S. Franzen, M.F. Davis, R.C. Oliver, J.K. Krueger, Dehaloperoxidase–hemoglobin from amphitrite ornata is primarily a monomer in solution, J. Phys. Chem. B 115 (2011) 4266–4272.

[2] S. Franzen, M.K. Thompson, R.A. Ghiladi, The dehaloperoxidase paradox, Biochim. Biophys. Acta 2012 (1824) 578–588.

[3] L. Lebioda, M.W. LaCount, E. Zhang, Y.P. Chen, K. Han, M.M. Whitton, D.E. Lincoln, S.A. Woodin, An enzymatic globin from a marine worm, Nature 401 (1999) 445.

[4] R.E. Weber, C. Mangum, H. Steinman, C. Bonaventura, B. Sullivan, J. Bonaventura, Hemoglobins of two terebellid polychaetes: *Enoplobranchus sanguineus* and *Amphitrite ornata*, Comp. Biochem. Physiol. A: Comp. Physiol. 56 (1977) 179–187.

[5] Y.P. Chen, S.A. Woodin, D.E. Lincoln, C.R. Lovell, An unusual dehalogenating peroxidase from the marine terebellid ploychaete *Amphitrite ornata*, J. Biol. Chem. 271 (1996) 4609–4612.

[6] J. Belyea, L.B. Gilvey, M.F. Davis, M. Godek, T.L. Sit, S.A. Lommel, S. Franzen, Enzyme function of the globin dehaloperoxidase from *Amphitrite ornate* is activated by substrate binding, Biochemistry 44 (2005) 15637–15644.

[7] R.L. Osborne, M.K. Coggins, G.M. Raner, M. Walla, J.H. Dawson, The mechanism of oxidative halophenol dehalogenation by *Amphitrite ornata* dehaloperoxidase is initiated by H_2O_2 binding and involves two consecutive one-electron steps: role of ferryl intermediates, Biochemistry 48 (2009) 4231–4238.

[8] S. Franzen, L.B. Gilvey, J.L. Belyea, The pH dependence of the activity of dehaloperoxidase from *Amphitrite ornata*, Biochim. Biophys. Acta, Proteins Proteomics 1774 (2007) 121–130.

[9] J.J. Zhao, J. Rowe, J. Franzen, C. He, S. Franzen, Study of the electrostatic effects of mutations on the surface of dehaloperoxidase-hemoglobin A, Biochem. Biophys. Res. Commun. 420 (2012) 733–737.

[10] H.A. Ma, M.K. Thompson, J. Gaff, S. Franzen, Kinetic analysis of a naturally occurring bioremediation enzyme: dehaloperoxidase-hemoglobin from *Amphitrite ornata*, J. Phys. Chem. B 114 (2010) 13823–13829.

[11] S.S. Andrews, S.G. Boxer, Vibrational Stark effects of nitriles I. Methods and experimental results, J. Phys. Chem. A 104 (2000) 11853–11863.

[12] S.H. Brewer, S. Franzen, A quantitative theory and computational approach for the vibrational Stark effect, J. Chem. Phys. 119 (2003) 851–858.

[13] S.G. Boxer, Stark realities, J. Phys. Chem. B 113 (2009) 2972–2983.

[14] G. Schkolnik, J. Salewski, D. Millo, I. Zebger, S. Franzen, P. Hildebrandt, Vibrational Stark effect of the electric-field reporter 4-mercaptobenzonitrile as a tool for investigating electrostatics at electrode/SAM/solution interfaces, Intl. J. Mol. Sci. 13 (2012) 7466–7482.

[15] A.T. Fafarman, P.A. Sigala, J.P. Schwans, T.D. Fenn, D. Herschlag, S.G. Boxer, Quantitative, directional measurement of electric field heterogeneity in the active site of ketosteroid isomerase, Proc. Natl. Acad. Sci. USA 109 (2012) E299–E308.

[16] I.T. Suydam, S.G. Boxer, Vibrational Stark effects calibrate the sensitivity of vibrational probes for electric fields in proteins, Biochemistry 42 (2003) 12050–12055.

[17] V. Oklejas, C. Sjostrom, J.M. Harris, SERS detection of the vibrational stark effect from nitrile-terminated SAMs to probe electric fields in the diffuse double-layer, J. Phys. Chem. B 124 (2002) 2408–2409.

[18] A.J. Stafford, D.L. Ensign, L.J. Webb, Vibrational Stark effect spectroscopy at the interface of Ras and Rap1A bound to the Ras binding domain of RalGDS reveals an electrostatic mechanism for protein–protein interaction, J. Phys. Chem. B 114 (2010) 15331–15344.

[19] M.M. Waegele, R.M. Culik, F. Gai, Site-specific spectroscopic reporters of the local electric field, hydration, structure, and dynamics of biomolecules, J. Phys. Chem. Lett. 2 (2011) 2598–2609.

[20] N.M. Levinson, S.D. Fried, S.G. Boxer, Solvent-induced infrared frequency shifts in aromatic nitriles are quantitatively described by the vibrational Stark effect, J. Phys. Chem. B 116 (2012) 10470–10476.

[21] G. Schkolnik, T. Utesch, J. Salewski, K. Tenger, D. Millo, A. Kranich, I. Zebger, C. Schulz, L. Zimanyi, G. Rakhely, M.A. Mroginski, P. Hildebrandt, Mapping local electric fields in proteins at biomimetic interfaces, Chem. Commun. 48 (2012) 70–72.

[22] H. Jo, R.M. Culik, I.V. Korendovych, W.F. DeGrado, F. Gai, Selective incorporation of nitrile-based infrared probes into proteins via cysteine alkylation, Biochemistry 49 (2010) 10354–10356.

[23] V. de Serrano, Z.X. Chen, M.F. Davis, S. Franzen, X-ray crystal structural analysis of the binding site in the ferric and oxyferrous forms of the recombinant heme dehaloperoxidase cloned from *Amphitrite ornata*, Acta Crystallogr., Sect. D: Biol. Crystallogr. 63 (2007) 1094–1101.

[24] W. Humphrey, A. Dalke, K. Schulten, VMD: Visual molecular dynamics, J. Mol. Graphics 14 (1996) 33–38.

[25] W.L. Jorgensen, J. Chandrasekhar, J.D. Madura, R.W. Impey, M.L. Klein, Comparison of simple potential functions for simulating liquid water, J. Chem. Phys. 79 (1983) 926–935.

[26] M.K. Thompson, S. Franzen, R.A. Ghiladi, B.J. Reeder, D.A. Svistunenko, Compound ES of dehaloperoxidase decays via two alternative pathways depending on the conformation of the distal histidine, J. Am. Chem. Soc. 132 (2010) 17501–17510.

[27] A.D. MacKerell, D. Bashford, M. Bellott, R.L. Dunbrack, J.D. Evanseck, M.J. Field, S. Fischer, J. Gao, H. Guo, S. Ha, D. Joseph-McCarthy, L. Kuchnir, K. Kuczera, F.T.K. Lau, C. Mattos, S. Michnick, T. Ngo, D.T. Nguyen, B. Prodhom, W.E. Reiher, B. Roux, M. Schlenkrich, J.C. Smith, R. Stote, J. Straub, M. Watanabe, J. Wiorkiewicz-Kuczera, D. Yin, M. Karplus, All-atom empirical potential for molecular modeling and dynamics studies of proteins, J. Phys. Chem. B 102 (1998) 3586–3616.

[28] J.C. Phillips, R. Braun, W. Wang, J. Gumbart, E. Tajkhorshid, E. Villa, C. Chipot, R.D. Skeel, L. Kale, K. Schulten, Scalable molecular dynamics with NAMD, J. Comput. Chem. 26 (2005) 1781–1802.

[29] S.E. Feller, Y.H. Zhang, R.W. Pastor, B.R. Brooks, Constant pressure molecular dynamics simulation - the Langevin Piston method, J. Chem. Phys. 103 (1995) 4613–4621.

[30] W.F. Van Gunsteren, H.J.C. Berendsen, Algorithms for macromolecular dyancmis and constraint dynamics, Mol. Phys. 34 (1977) 1311–1327.

[31] T. Darden, D. York, L. Pedersen, Partice Mesh Ewald - An N log(N) method for Ewald sums in large systems, J. Chem. Phys. 98 (1993) 10089–10092.

[32] A. Ghosh, A. Remorino, M.J. Tucker, R.M. Hochstrasser, 2D IR photon echo spectroscopy reveals hydrogen bond dynamics of aromatic nitriles, Chem. Phys. Lett. 469 (2009) 325–330.

[33] D.J. Aschaffenburg, R.S. Moog, Probing hydrogen bonding environments: solvatochromic effects on the CN vibration of benzonitrile, J. Phys. Chem. B 113 (2009) 12736–12743.

[34] S.D. Dalosto, J.M. Vanderkooi, K.A. Sharp, Vibrational Stark effects on carbonyl, nitrile, and nitrosyl compounds including heme ligands, CO., CN, and NO, studied with density functional theory, J. Phys. Chem. B 108 (2004) 6450–6457.

[35] S.D. Dalosto, N.V. Prabhu, J.M. Vanderkooi, K.A. Sharp, A density functional theory study of conformers in the ferrous CO complex of horseradish peroxidase with distinct Fe–C–O configurations, J. Phys. Chem. B 107 (2003) 1884–1892.

[36] M.K. Thompson, M.F. Davis, V. de Serrano, F.P. Nicoletti, B.D. Howes, G. Smulevich, S. Franzen, Internal binding of halogenated phenols in dehaloperoxidase-hemoglobin inhibits peroxidase activity, Biophys. J. 99 (2010) 1586–1595.